


RESEARCH ARTICLE

Strong coupling between an optical microcavity and photosystems in single living cyanobacteria

Tim Rammler^{1,2} | Frank Wackenhut^{1*}  | Sven zur Oven-Krockhaus^{1,2} |
Johanna Rapp³ | Karl Forchhammer³ | Klaus Harter² | Alfred J. Meixner^{1*}

¹Institute of Physical and Theoretical Chemistry, University of Tübingen, Tübingen, Germany

²Center for Plant Molecular Biology, University of Tübingen, Tübingen, Germany

³Interfaculty Institute of Microbiology and Infection Medicine, University of Tübingen, Tübingen, Germany

***Correspondence**

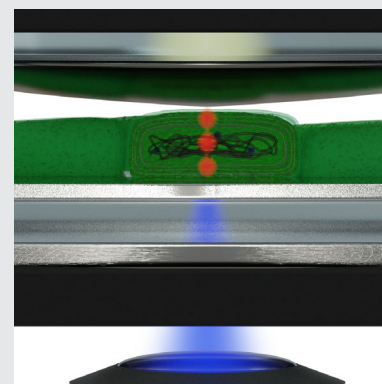
Frank Wackenhut and Alfred J. Meixner, Institute of Physical and Theoretical Chemistry, University of Tübingen, Tübingen, Germany.
Email: frank.wackenhut@uni-tuebingen.de (F. W.) and alfred.meixner@uni-tuebingen.de (A. J. M.)

Funding information

Deutsche Forschungsgemeinschaft, Grant/Award Numbers: SFB 1101/Z02, SFB 1101/D02, HA 2146/23-1, ME 1600/13-3; VW foundation

Abstract

The first step in photosynthesis is an extremely efficient energy transfer mechanism that led to the debate to which extent quantum coherence may be involved in the energy transfer between the photosynthetic pigments. In search of such a coherent behavior, we have embedded living cyanobacteria between the parallel mirrors of an optical microresonator irradiated with low intensity white light. As a consequence, we observe vacuum Rabi splitting in the transmission and fluorescence spectra as a result of strong light matter coupling of the chlorophyll *a* molecules in the photosystems (PSs) and the cavity modes. The Rabi-splitting scales with the number of the PSs chlorophyll *a* pigments involved in strong coupling indicating a delocalized polaritonic state. Our data provide evidence that a delocalized polaritonic state can be established between the chlorophyll *a* molecule of the PSs in living cyanobacterial cells at ambient conditions in a microcavity.



1 | INTRODUCTION

In photosynthesis, light energy is absorbed and converted into relatively stable chemical products by well organized, dynamic, membrane-integral pigment-protein complexes called photosystems for long-term chemical energy storage.^{1,2} Photosynthetic complexes are optimized to capture photons from solar light and transmit the excitation energy from peripheral pigments to the photosynthetic reaction center with an extremely high efficiency (close to 100%³). They consist of a collection of pigment molecules, such as chlorophylls and carotenoids

that are arranged by a protein scaffold in a way that near-field dipole coupling is possible.³ When interacting with light they no longer act as independent excited molecules, but coupling between them results in collective excitations called excitons, whose wave function extends over several pigment units.^{4,5}

The observation of oscillatory intensity modulations of ultrafast photon echoes from isolated photosynthetic complexes of *Chlorobium* at cryogenic temperatures and under almost physiological conditions led to the hypothesis that quantum coherence could be a possible explanation for the efficient energy transfer.^{4,6–10} Recent investigations

This is an open access article under the terms of the Creative Commons Attribution License, which permits use, distribution and reproduction in any medium, provided the original work is properly cited.

© 2021 The Authors. *Journal of Biophotonics* published by Wiley-VCH GmbH.

have revealed that both electronic and vibrational coherences are involved in primary energy transfer in bacterial reaction centers.^{11,12} However, excitation in ultrafast time-resolved laser spectroscopy, as it was done in the experiments mentioned above, is pulsed and coherent, while perception of white light under ambient conditions occurs continuously over the course of minutes to hours via incoherent photons. As a consequence, the energy transfer in the photosynthetic machinery must operate on the basis of independent single photons. A possible alternative way to ultrashort laser pulses in time domain spectroscopy is to observe coherent light-matter interaction in the frequency domain by placing the respective chromophores in a resonant optical microresonator to achieve hybrid light-matter states.¹³ Thus, we have enclosed living cyanobacteria (*Synechococcus elongatus*) in the confined electromagnetic field between the two mirrors of the microresonator to probe their optical properties in vivo. Using low intensity white light irradiation, we

actually observe a symmetric splitting of the transmission band, which is a consequence of coherent excitonic coupling between the chlorophyll *a* pigments within photosystems (PSs) and the cavity field via the formation of a delocalized polaritonic state in vivo. We suspect that this coupling could lead to an explanation for the very efficient photosynthetic energy transfer within the PSs of cyanobacteria.

2 | RESULTS

To study possible quantum effects in the PSs of living organisms at ambient conditions, we embedded cells of *S. elongatus* (strain PCC 7942) in an optical microcavity. In contrast to sulfur bacteria,^{4,14} *S. elongatus* performs oxygenic photosynthesis. The photosynthesis of this cyanobacterial species is intensively studied with respect to biochemistry, structural organization and dynamics

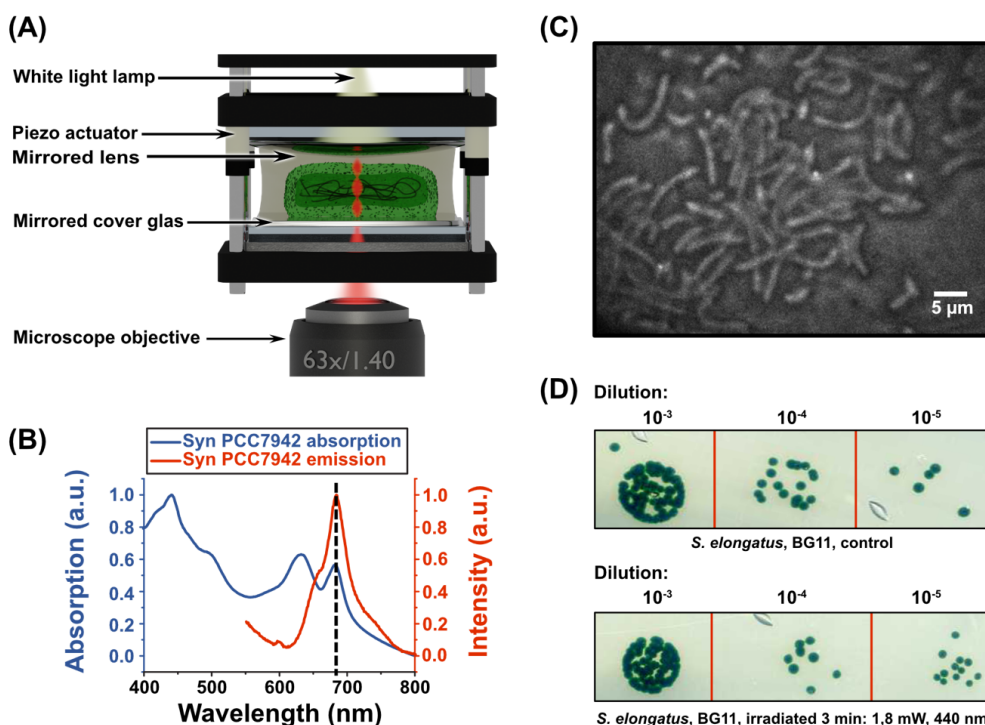


FIGURE 1 The spectral properties of the photosynthetic pigments of *S. elongatus* cells and a Fabry-Pérot microresonator. The survival of *S. elongatus* cells is not impaired by the light conditions prevailing in the microcavity. (A) Scheme of the Fabry-Pérot microcavity, which consists of two partially transparent mirrors. The distance between the mirrors can be fine-tuned with piezoelectric actuators. Due to constructive and destructive interference, only wavelengths fulfilling the resonance condition of the cavity are transmitted. The bacteria are placed in an agarose matrix inside the cavity. (B) Normalized absorption (blue) and fluorescence (red) spectra ($\lambda_{\text{ex}} = 440 \text{ nm}$) of *S. elongatus* cells located inside the microcavity. The dashed black line indicates the wavelength where the bacteria emit and absorb photons of the same wavelength. (C) Light microscopy image of *S. elongatus* cells inside the microcavity. (D) Spot assay¹⁶ of *S. elongatus* cells in BG11 medium. Top: Non-irradiated control in a dilution series (1:10), initial concentration: $\text{OD}_{750} = 0.5$. Below: Irradiated sample in a dilution series (1:10), initial concentration: $\text{OD}_{750} = 0.5$. The bacteria were irradiated with an expanded laser beam at adjusted intensity before the preparation of a spot assay. The irradiation conditions were comparable to those in the microcavity. The comparable growth rate indicates a negligible impact of the typical irradiation during the experiments

of the photosynthetic machinery^{1,15} and therefore well-suited for the study of quantum physical processes in vivo at ambient conditions.

Our Fabry-Pérot optical microresonator (quality factor, $Q = 98$) consists of two partially transparent mirrors (Figure 1A). Their distance can be precisely adjusted with a piezo actuator to control the resonance condition of the microcavity. Compared to previous works,¹⁴ we have chosen silver mirrors with a large layer thickness to achieve a stronger interaction between the microcavity and the cyanobacteria. More details about the experimental set up are given in the supporting information (Appendix S1). Transmission spectra were acquired from below via a high numerical aperture (NA) objective lens ($NA = 1.4$), while the microcavity was irradiated by a continuously emitting white light source from above (Figure 1A). Additionally, we irradiated the sample with a laser from below to detect strong coupling in the emission spectrum of individual bacteria, which is made possible by the small focal spot size of the high NA objective. As shown in Figure 1B, the in vivo absorption (blue line) shows the typical chlorophyll *a* maximum at around 680 nm due to a red-shift of protein-bound chlorophyll.¹⁷ The emission spectrum at 440 nm excitation reveals again a maximum at around 680 nm. This fluorescence emission can be predominantly assigned to the chlorophyll *a* pigments of the PSs as the fluorescence of the phycobilisomes is almost completely quenched in vivo.^{15,18,19} However, the observed fluorescence emission can predominantly be attributed to the chlorophyll *a* molecules of photosystem 2 (PS2), as the photosystem 1 (PS1) acts as a very efficient energy trap at ambient temperature.²⁰ The cavity resonance can be tuned across the absorption and emission maximum (see Figure S1), allowing efficient optical coupling between the cavity modes and the cyanobacteria. Remarkably, the absorption and emission spectra of the photosynthetic pigments largely overlap in the 680 nm region (Figure 1B), demonstrating that the cyanobacteria are able to reabsorb their own emitted light. This photophysical feature of *S. elongatus* is a prerequisite for the potential coupling of the photosynthetic pigments to an optical field confined in a microcavity.

The survival rate of the cyanobacteria in the microcavity was assayed to examine the possible impact of the laser irradiation on the embedded organisms (Figure 1C). Since only a single bacterium is exposed to the focused laser irradiation inside the cavity at a time, which cannot be isolated after the experiment, we have designed an assay to analyze comparable irradiation conditions by embedding a cyanobacterial culture in a low-melting agarose matrix outside the cavity. The cyanobacteria were then exposed to light conditions (440 nm, 1000 $\mu\text{mol photons s}^{-1} \text{m}^{-2}$, 3 minutes) similar to those

prevailing in the cavity, while a non-irradiated culture served as a control and the survivability was analyzed by a spot assay (see supporting information [Appendix S1] for details). No growth difference between the irradiated and non-irradiated sample was observed (Figure 1D), indicating that the light conditions in the microcavity have no discernible impact on the cyanobacterial survivability.

To determine whether the microcavity influences the cyanobacterial photosynthetic system in vivo, fluorescence lifetimes (FLTs)²¹ of its pigments in single bacteria were acquired.

The light-harvesting pigments of the PSs serve to rapidly and efficiently transfer light energy from the peripheral pigments to the reaction center, therefore, the fluorescence signal of cyanobacteria is weak. Transfer and trapping of the excitation energy in the PSs lead to a fast non-exponential fluorescence decay, which can be observed from live cyanobacteria with a wide distribution of FLT components from short ones in the low and mid picosecond range and slow components in the low nanosecond range.²² The spontaneous emission rate of a chromophore can be increased or decreased by placing it in a microcavity and tuning it in-resonance or off-resonance with the chromophore emission. This is known as Purcell effect^{23,24} leading to shorter or longer FLTs, respectively. The long-lived FLT component originates from particularly those PS2 chlorophyll *a* pigments where the excitation energy is trapped in an emitting state and can therefore be analyzed in vivo for three cases: (a) free space (outside of the cavity), (b) inside the cavity in off-resonance mode and (c) inside the cavity in resonance mode. Due to the extreme efficient energy transfer of PS1, its FLT is around 20 ps,²⁵ which is much shorter than the temporal resolution of the used time correlated single photon counting equipment. Hence, we assume that the observed FLTs are those of PS2. Short laser pulses ($\lambda_{ex} = 440 \text{ nm}$) with pulse durations of less than 80 ps and a pulse rate of 80 MHz were used. The PS2 chlorophyll *a* pigments irradiated in free space (i) reveal a FLT value of $\tau_I = (0.26 \pm 0.006) \text{ ns}$ ((i) in Figure 2) and a slightly larger value of $\tau_I = (0.29 \pm 0.016) \text{ ns}$ in the off-resonant microcavity ((ii) in Figure 2). In contrast, the FLT of the PS2 pigments in the resonant microcavity (iii) decreased to $\tau_I = (0.16 \pm 0.006) \text{ ns}$ and was significantly shorter compared with the data obtained in free space or in the off-resonant cavity. This result is consistent with the Purcell effect²³ of isolated pigments and demonstrates that the microcavity has a noticeable impact on the PS2 photosynthetic processes in single living cyanobacteria.

In general, the interaction of a quantum system with the optical field in a microcavity can be separated in the weak and strong coupling regime. In the weak coupling regime, the individual damping constants of the cavity

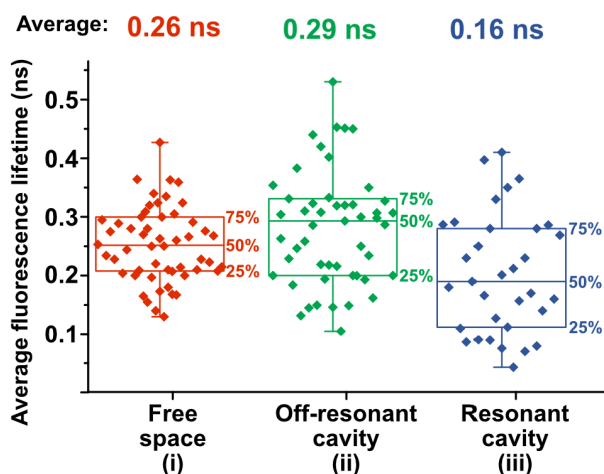


FIGURE 2 The FLT of *S. elongatus* chlorophyll *a* pigments is influenced in vivo by the microcavity. The bacteria were embedded in low-melting agarose and irradiated with short laser pulses ($\lambda_{\text{ex}} = 440$ nm) with a duration of less than 80 ps and a repetition rate of 80 MHz. The average intensity-weighted FLTs were recorded in free space ([a], red, $n = 53$), inside the off-resonance cavity ([b], green, $n = 50$) or inside the cavity in resonance with the light emission of the cyanobacteria ([c], blue, $n = 33$). The center line in the box plot indicates the median, box edges show the 75th and 25th percentiles, and whiskers cover the full range of values. A two-tailed t-test confirms a significant difference between the PS2 chlorophyll *a* FLTs for the off-resonant (and without) cavity and the resonant cavity, $p = 2.05 \times 10^{-5}$, ($p = 3.20 \times 10^{-6}$)

and the chlorophyll *a* pigments are larger than the coupling constant. In this case, the microcavity only influences the spontaneous emission rate via the Purcell effect as observed in the FLT analysis (Figure 2). However, if the coupling constant exceeds the individual damping constants, the energy of a photon can be coherently cycled back and forth between the oscillating electromagnetic field in the microcavity and the induced polarization formed by a large number of coherent electronically excited chromophores enclosed between the cavity mirrors before it escapes from the cavity; this condition reflects the strong coupling regime.²⁶ The energy of the photon, which is dispersed in the whole mode volume and shared between the cavity mode and the polarization, is described in quantum electrodynamics as a hybrid light-matter state or polariton.^{27–29} In our case, these so-called polaritonic modes are a coherent superposition of the cavity mode and the electronically excited state of the chlorophyll *a* pigments in the PSs. As shown in Figure S2, the back and forth cycling of the photon energy between the electromagnetic field in the microcavity and the polarization in the time domain leads to a splitting in the spectral domain that manifests itself as a double-peaked cavity transmission spectrum with a peak separation referred to as vacuum Rabi splitting, as schematically illustrated in Figure 3A,B.

To study vacuum Rabi splitting, due to a polaritonic mode in the PSs of a living cyanobacterium and the optical field in the microcavity, we simulated and experimentally investigated the dispersive behavior of the coupled system.

The dashed lines in Figure 3A,B illustrate the simulated uncoupled emission of the cyanobacteria PSs (green) and the cavity mode (red). Figure 3A illustrates the case when there is no spectral overlap between them. The transmission spectrum of such a coupled, but off-resonant system, is similar to that of the uncoupled cavity mode. Conversely, when the cavity mode approaches the spectral position of the chlorophyll *a* emission, a splitting into two polaritonic modes is visible (Figure 3B, blue line). Figure 3C represents the simulated spectral shift $\Delta\lambda$ of the coupled modes relative to the uncoupled modes. The shift caused by strong coupling is largest when the cavity is in resonance with the chlorophyll *a* emission, leading to a symmetric double-peaked cavity transmission spectrum. The occurrence of such a spectral gap between the two polaritonic modes is called vacuum Rabi splitting. Mathematically, such a coupled system can be modeled by two coupled damped harmonic oscillators, as described in the supporting information (Appendix S1) or in Reference 30. First, we want to illustrate in Figure 3D, E the results of the calculation without coupling between the cavity mode and the chlorophyll *a* emission ($\kappa = 0$ eV). Each line in Figure 3D represents a cavity transmission spectrum, as indicated by the spectrum number, and its intensity is given by the color map. In this simulation, the cavity length gradually increased from top to bottom, leading to a spectral red shift of the cavity resonance. The dashed lines in Figure 3D,E represent the spectral position of the uncoupled chlorophyll *a* emission and the cavity mode, respectively. In the absence of strong coupling, no splitting is observed, even when both modes were tuned to the same resonance wavelength; the chlorophyll *a* emission was only influenced by the Purcell effect (Figure 3E). This changes with strong coupling between the cavity mode and the chlorophyll *a* pigments, with a calculated coupling constant of $\kappa = 0.14$ eV in Figure 3F,G. The calculated cavity transmission spectra in Figure 3F show a clear anti-crossing behavior when the cavity resonance approaches the spectral position of the chlorophyll *a* emission at 680 nm. In the calculated emission spectra in Figure 3G, the mode splitting is less obvious, because it is obscured by the spectrally broad fluorescence background of the chlorophyll *a* pigments that are not strongly coupled to the cavity mode. The uncoupled chlorophyll *a* pigments have their electronic transition dipole moments oriented perpendicular to the polarization and constitute about 2/3 of the total number of chlorophyll *a* pigments. By comparing the simulations in Figure 3D,E with Figure 3F,G, it is

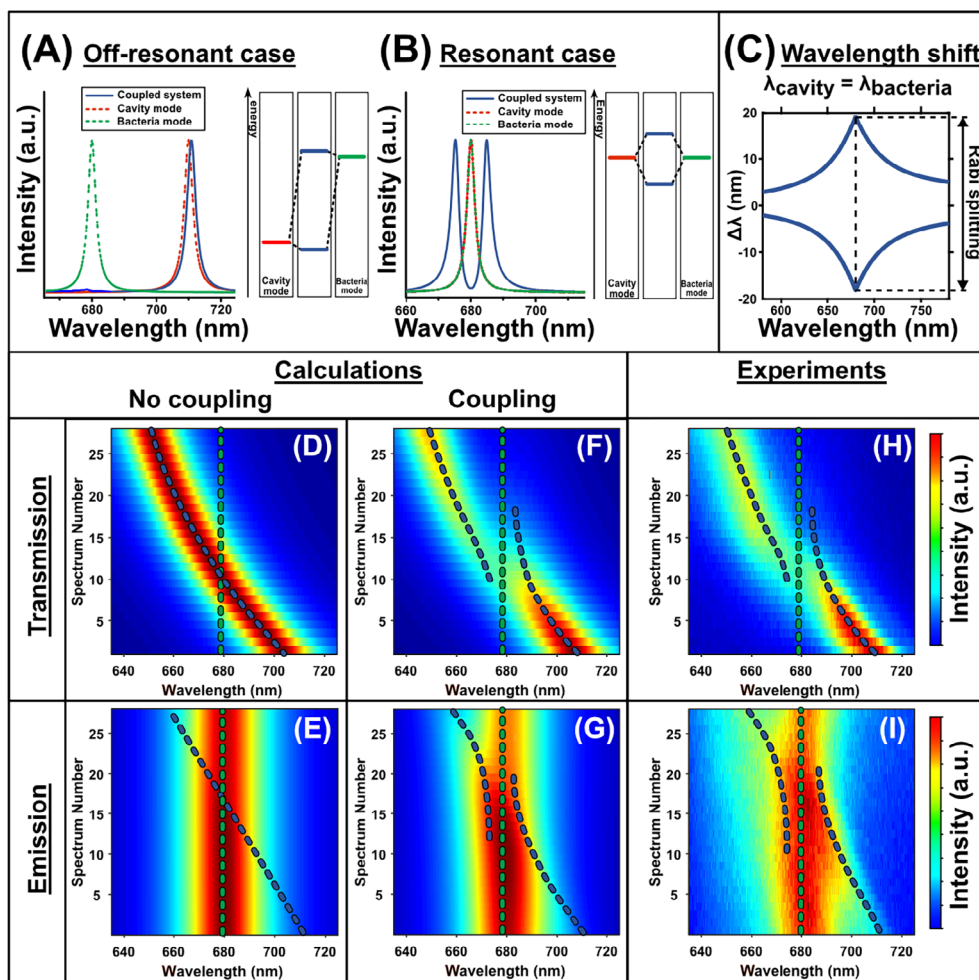


FIGURE 3 Strong coupling between a microcavity and the chlorophyll *a* pigments in living cyanobacteria. (A) represents where the bacteria absorption/emission and the cavity are spectrally separated. The dashed green and red spectra represent the uncoupled bacteria absorption/emission mode and cavity mode. The blue spectrum illustrates the cavity transmission spectrum for the nonresonant but coupled case and is similar to the uncoupled system. The graph on the right illustrates the corresponding energy level scheme. (B) Illustration of the resonant case, where the cavity mode is spectrally overlapping with the emission of the PSs, and two polaritonic modes (blue lines) are clearly visible in the double-peaked cavity transmission spectrum. (C) Spectral shift $\Delta\lambda$ of the coupled modes relative to the uncoupled ones. The largest splitting, that is, vacuum Rabi splitting, is observed when the cavity and the chlorophyll *a* pigments of the cyanobacterial PSs are in resonance. (D,E) Simulated cavity transmission/ bacteria emission spectra without coupling as a function of the decreasing mirror distance (indicated by the spectrum number). The dashed green and blue lines are the spectral position of the uncoupled bacteria emission/ cavity resonance, respectively. No anti-crossing can be observed when the cavity mode is tuned across the chlorophyll *a* emission. (F,G) Simulated cavity transmission/ chlorophyll *a* emission spectra including strong coupling between the cavity mode and the emission. Strong coupling is visible in (F,G) by the anti-crossing dispersion, when the cavity mode is close to the emission of the cyanobacterial PSs. (H,I) Experimental cavity transmission/ chlorophyll *a* emission spectrum. Strong coupling can be observed in (H,I) by the anti-crossing dispersion and is in perfect agreement with the simulation in (F,G)

possible to experimentally distinguish between no/weak and strong coupling in the microcavity-cyanobacterial system. Notably, the experimental white light transmission spectra derived from the PSs of living cyanobacteria show a clear anti-crossing behavior when the cavity resonance is tuned over the chlorophyll *a* emission at 680 nm (Figure 3H). In the emission spectra (Figure 3I) the splitting is less obvious since it is composed of two types of photons, those that participate in the strong coupling process with the cavity mode and those that escape from

the resonator without coupling due to the Purcell effect. The experimental results fit perfectly to the calculated spectra in Figure 3F,G and prove that strong coupling between the microcavity and the chlorophyll *a* pigments is achievable in living cyanobacteria.

According to the Jaynes-Cummings model, the energy splitting ΔE is given by Equation (1) and is proportional to the square root of the number n of chlorophyll *a* pigments that coherently couple to the cavity mode with a coupling constant g_0 .²⁶

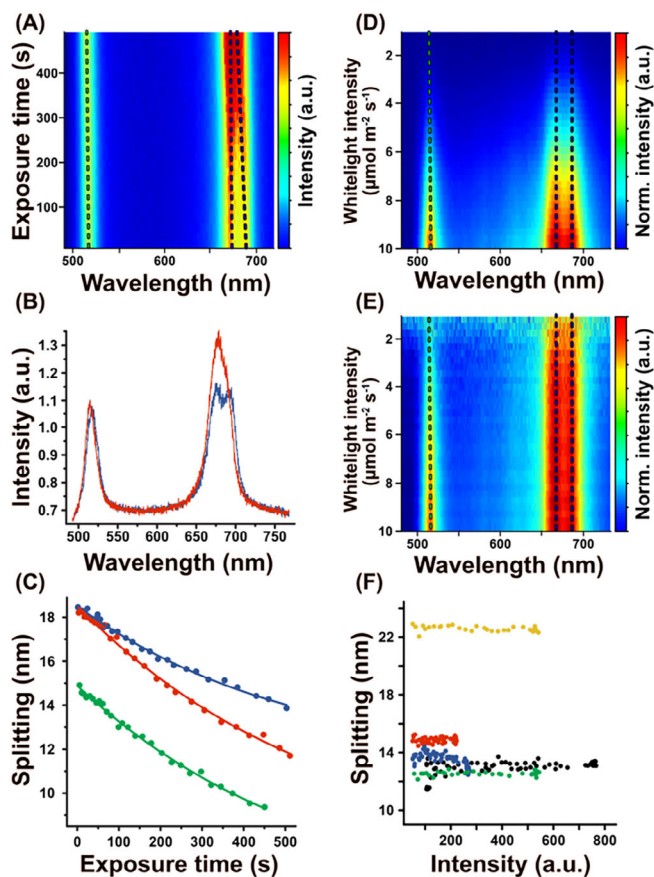


FIGURE 4 Reducing the number of chlorophyll *a* pigments in a cyanobacterium by photobleaching reduces vacuum Rabi splitting and shows that the chlorophyll *a* pigments are coherently coupled in living cyanobacterial cells. (A) Cavity transmission spectra with two cavity modes as a function of the exposure time. One mode shows vacuum Rabi splitting (dashed blue line), while the other is not coupled (dashed green line). The splitting energy, and thus the coupling, is reduced by the continuous irradiation and photobleaching the chlorophyll *a* pigments of the bacterium. (B) First (blue line, $t = 0$ s) and last (red line, $t = 500$ s) spectrum of A. (C) Rabi splitting between the two intensity maxima around 680 nm as a function of the exposure time. Three different, individual bacteria (red, green and blue) in the cavity show the decrease of the vacuum Rabi splitting with increasing bleaching of the chlorophyll *a* pigments. (D) Cavity transmission spectra with two resonances as a function of the illumination intensity of the white light lamp of $10 \mu\text{mol photons s}^{-1} \text{m}^{-2}$ to $1 \mu\text{mol photons s}^{-1} \text{m}^{-2}$ (corresponding to $28 - 2.8 \text{ mWcm}^{-2}$ at 680 nm) from bottom to top. The coupling remains constant while the intensity of the white light lamp is reduced. (E) Intensity normalized version of (D), where each spectrum is normalized to its maximum intensity, to better visualize the constant splitting. (F) Splitting as a function of the white light intensity. At low illumination intensity, five different, individual bacteria in the cavity show that the vacuum Rabi splitting is independent of the light intensity

$$\Delta E = 2\sqrt{n}\hbar g_0 \quad (1)$$

Therefore, the splitting energy should decrease when the number of pigments is reduced. This can indeed be

achieved in a living cyanobacterium by photobleaching a fraction of the functional chlorophyll *a* pigments by increasing the laser intensity by a factor of 100 as compared to the previous experiments.

As shown in Figure 4A at the beginning the cavity mode at $\lambda = 680$ nm had a spectral dip at the center due to vacuum Rabi splitting. As the photobleaching of the chlorophyll *a* molecules proceeded (Figure 4A, blue dashed line), the energy splitting between the two peaks reduced and disappeared. In contrast, at the same time for the cavity mode at $\lambda = 546$ nm, which has no coupling to the chlorophyll *a* pigments, no changes in intensity or spectral position were visible. This is further illustrated in Figure 4B, where the first (blue line) and the last (red line) spectrum of the spectral series in Figure 4A are shown.

The number of molecules (n in Equation (1)) decreased exponentially by photobleaching as tested at three different locations in the cavity, resulting in a decreased splitting of the coupled modes, which can be fitted to the square root of an exponential decay (Figure 4C). These results demonstrate that the extent of the Rabi splitting depends on the number of chlorophyll *a* pigments effectively participating in polaritonic coupling to the optical mode throughout the entire focal volume.

To reveal the light intensity dependence, white-light transmission spectra were acquired with different excitation intensities of $10 \mu\text{mol photons s}^{-1} \text{m}^{-2}$ down to $1 \mu\text{mol photons s}^{-1} \text{m}^{-2}$ (corresponding to $28.0 - 2.8 \text{ mWcm}^{-2}$ measured at 680 nm) in single living cyanobacteria as shown in Figure 4D,E, where the y-axis corresponds to different excitation intensities. The resonance mode at $\lambda = 680$ nm, which is strongly coupled to chlorophyll *a*, showed Rabi splitting which remained constant with decreasing white light irradiation intensity (Figure 4D). This was even more obvious in the normalized spectra (Figure 4E), where each spectrum along the y-axis was normalized to its maximum intensity. This constant Rabi splitting was observed for different individual cyanobacteria in the sample, as shown in Figure 4F by plotting the Rabi splitting against the intensity of the cavity mode. As a consequence, since the photons used for white-light illumination are completely incoherent, strong coupling must occur even at very low light intensity; or in other words, one resonant photon is already sufficient to induce a polaritonic state between the microcavity and the chlorophyll *a* pigments in vivo.

3 | DISCUSSION

The emission and transmission spectra presented here suggest that there is in vivo strong coupling between the microcavity and the chlorophyll *a* pigments of the

cyanobacterial photosystem. Photo-bleaching experiments confirm that the microcavity couples to about 4.8×10^5 chlorophyll *a* molecules (calculated from the measured splitting and assuming that a chlorophyll molecule has a transition dipole moment of $5.39D$ and that the average refractive index of its surroundings is $n = 1.34$,³¹ see supporting information [Appendix S1] for calculation) at the same time to form a delocalized polaritonic state. Considering that each PS2 monomer contains 35 chlorophyll *a* molecules and each PS1 monomer 96 chlorophyll *a* molecules^{32,33} the experimentally determined coupling of 4.8×10^5 chlorophyll *a* molecules suggests that the majority of the PS bound chlorophyll *a* pigments in the thylakoid membrane of a cyanobacterial cell participate to the interaction with the microcavity. The term vacuum Rabi splitting refers to number of photons in the resonator, which can be zero, indicating that it works at very low light intensities and for the formation of a polaritonic state one single photon is sufficient. The wide delocalization of the polaritonic state suggests that each PS reaction center is optimally supplied with photons also in a low-light environment. To be able to take advantage of the long-range polaritonic state, a complex and dynamic spatial and structural organization of the PS complexes appears to be required, which compensates or makes use of the thermodynamic fluctuations occurring in the ambient environment. The functional implications on the physiology of oxygenic photosynthetic organisms have to be determined in future, involving molecular genetic approaches. However, our observation of strong coupling between the photosynthetic light harvesting machinery of living cyanobacteria and an optical microcavity at ambient conditions makes it worth investigating other biological processes, which are difficult to be explained by classical thermodynamics with respect to quantum electrodynamics effects.^{3,34} Future experiments will show if and to what degree the semi-classical model of energy “hopping” in the light-harvesting machinery of PSs must be expanded by a delocalized wave-like energy transfer under natural irradiation conditions.

4 | METHODS

4.1 | Preparation of cavity mirrors

The mirrors were produced by evaporating a 3 nm thick chromium layer on a glass surface serving as an adhesion layer for the following silver layer, which has a thickness of 30 nm or 60 nm for the lower and upper mirror, respectively. Since silver is bactericidal and very susceptible to damage and oxidation, it was coated with a gold layer (5 nm) and an SiO₂ layer (20 nm).³⁵ These layer

thicknesses result in a microcavity with a quality factor of $Q = 98$. The microcavity was assembled in a custom-built holder with piezo actuators and mounted on a stage scanning confocal microscope for the collection of both white light transmission and fluorescence spectra from the same spatial position.

4.2 | Light intensity measurements

The light intensity was measured with a Li-Cor Li-189 radiometer from Heinz Walz GmbH (Germany).

4.3 | Bacterial cultivation conditions

Synechococcus elongatus PCC 7492 cells were cultivated under photoautotrophic conditions with continuous illumination at around $30 \mu\text{mol photons s}^{-1} \text{m}^{-2}$ (Lumilux de Lux, Daylight, Osram) at 28°C. The cultures were grown in 100 mL Erlenmeyer flasks, filled with 40 mL BG11³⁶ medium, supplemented with 5 mM NaHCO₃ and shaken at 120 – 130 rpm.

4.4 | The survivability after laser irradiation analyzed by a spot assay

The *S. elongatus* cultures of both treatments were adjusted to an optical density $\text{OD}_{750} = 0.5$, and a dilution series to the power of 10 was made in BG11 medium ($10^0 - 10^{-5}$). Five microliters of each dilution was dropped on BG11-agar plates and cultivated at 28°C³⁷ under constant light with the intensity of $30 \mu\text{mol photons s}^{-1} \text{m}^{-2}$ for 7 days. All experiments are shown in Figure 1D. Top: Non-irradiated control in a dilution series (1:10), three replicates. Figure 1D below: Irradiated sample in a dilution series (1:10), three replicates. The bacteria were irradiated with a lens widened laser beam at adjusted intensity ($\lambda_{\text{ex}} = 440 \text{ nm}$, power: 1.8 mW) for 3 minutes before preparation of a spot assay. Representative results are shown in Figure 1D.

4.5 | The spectral properties of *S. elongatus*

To characterize the spectral properties of the photosynthetic pigments, absorption and emission spectra were recorded from 20 μL of a cyanobacterial suspension, embedded in a low-melting agarose matrix to prevent cell movement (Figure 1C). The absorption spectrum shown in Figure 1B features four distinct bands: the solet band of chlorophyll *a* at 440 nm,³⁸ the carotenoid band at

500 nm,³⁹ the PBS band at 630 nm⁴⁰ and the Q_y band of chlorophyll *a* at 680 nm.⁴¹ Excitation of the solet band is very efficient, taking additional advantage of the large Stokes shift to separate the laser reflection at the cavity mirrors from the emission signal, which is dominated by the chlorophyll *a* emission at 680 nm.³⁹

ACKNOWLEDGMENTS

The authors would like to thank F. de Courcy for English proofreading of the manuscript, M. Kittelberger for initial experiments and M. Harter for the hint of trying quantum biology. Alfred J. Meixner, Frank Wackenhut and Klaus Harter acknowledge support by the VW foundation (project title: A quantum beat for life) and the Deutsche Forschungsgemeinschaft (ME 1600/13-3; HA 2146/23-1; SFB 1101/D02, SFB 1101/Z02). Open access funding enabled and organized by Projekt DEAL.

AUTHOR CONTRIBUTIONS

Sven zur Oven-Krockhaus, Klaus Harter and Alfred J. Meixner designed the project. Tim Rammler and Johanna Rapp performed experiments. Tim Rammler and Frank Wackenhut analyzed the data and wrote the manuscript with input and proofreading from Karl Forchhammer, Klaus Harter, Alfred J. Meixner, Sven zur Oven-Krockhaus and Johanna Rapp.

DATA AVAILABILITY STATEMENT

Data are available in the main text or the supplementary materials. Further material is available from the corresponding author upon reasonable request.

ORCID

Frank Wackenhut  <https://orcid.org/0000-0001-6554-6600>

REFERENCES

- [1] S. Casella, F. Huang, D. Mason, G. Y. Zhao, G. N. Johnson, C. W. Mullineaux, L. N. Liu, *Mol. Plant* **2017**, *10*, 1434.
- [2] A. Stírbet, D. Lazár, Y. Guo, G. Govindjee, *Ann. Bot.* **2020**, *126*, 511.
- [3] G. R. Fleming, G. D. Scholes, Y.-C. Cheng, *Proc. Chem.* **2011**, *3*, 38.
- [4] G. S. Engel, T. R. Calhoun, E. L. Read, T. K. Ahn, T. Mančal, Y. C. Cheng, R. E. Blankenship, G. R. Fleming, *Nature* **2007**, *446*, 782.
- [5] J. Strümpfer, M. Şener, K. Schulten, *J. Phys. Chem. Lett.* **2012**, *3*, 536.
- [6] E. Collini, *Chem. Soc. Rev.* **2013**, *42*, 4932.
- [7] E. Collini, C. Y. Wong, K. E. Wilk, P. M. G. Curmi, P. Brumer, G. D. Scholes, *Nature* **2010**, *463*, 644.
- [8] Y.-C. Cheng, G. R. Fleming, *Annu. Rev. Phys. Chem.* **2009**, *60*, 241.
- [9] R. Hildner, D. Brinks, J. B. Nieder, R. J. Cogdell, N. F. van Hulst, *Science* **2013**, *340*, 1448.
- [10] P. D. Dahlberg, G. J. Norris, C. Wang, S. Viswanathan, V. P. Singh, G. S. Engel, *J. Chem. Phys.* **2015**, *143*, 101101.
- [11] J. Cao, R. J. Cogdell, D. F. Coker, H. G. Duan, J. Hauer, U. Kleinekathöfer, T. L. C. Jansen, T. Mančal, R. J. D. Miller, J. P. Ogilvie, V. I. Prokhorenko, T. Renger, H. S. Tan, R. Tempelaar, M. Thorwart, E. Thyryhaug, S. Westenhoff, D. Zigmantas, *Sci. Adv.* **2020**, *6*, eaaz4888.
- [12] F. Ma, E. Romero, M. R. Jones, V. I. Novoderezhkin, R. van Grondelle, *Nat. Commun.* **2019**, *10*, 933.
- [13] T. W. Ebbesen, *Acc. Chem. Res.* **2016**, *49*, 2403.
- [14] D. Coles, L. C. Flatten, T. Sydney, E. Hounslow, S. K. Saikin, A. Aspuru-Guzik, V. Vedral, J. K. H. Tang, R. A. Taylor, J. M. Smith, D. G. Lidzey, *Small* **2017**, *13*, 1701777.
- [15] S. Rexroth, M. M. Nowaczyk, M. Rögner, Cyanobacterial Photosynthesis: The Light Reactions. in *Modern Topics in the Phototrophic Prokaryotes: Metabolism, Bioenergetics, and Omics* (Ed: P. C. Haltenbeck), Springer International Publishing, Cham, Switzerland **2017**, p. 163.
- [16] A. Doerrich, A. Wilde, *BIO-Protoc.* **2015**, *5*, e1574.
- [17] C. S. French, J. S. Brown, M. C. Lawrence, *Plant Physiol.* **1972**, *49*, 421.
- [18] I. N. Stadnichuk, P. M. Krasilnikov, D. V. Zlenko, *Microbiology* **2015**, *84*, 101.
- [19] A. F. Bhatti, R. R. Choubey, D. Kirilovsky, E. Wientjes, H. van Amerongen, *Biochim. Biophys. Acta BBA Bioenerg.* **2020**, *1861*, 148255.
- [20] G. H. Krause, E. Weis, Chlorophyll Fluorescence and Photosynthesis: The Basics, *37*.
- [21] J. R. Lakowicz, *Principles of Fluorescence Spectroscopy*, Springer, NewYork **2006**.
- [22] M. Byrdin, I. Rimke, E. Schlodder, D. Stehlik, T. A. Roelofs, *Biophys. J.* **2000**, *79*, 992.
- [23] E. M. Purcell, Spontaneous Emission Probabilities at Radio Frequencies. in *Confined Electrons and Photons: New Physics and Applications* (Eds: E. Burstein, C. Weisbuch), Springer, Boston, MA **1995**, p. 839.
- [24] A. I. Chizhik, A. M. Chizhik, D. Khoptyar, S. Bär, A. J. Meixner, J. Enderlein, *Nano Lett.* **2011**, *11*, 1700.
- [25] E. G. Andrizhivskaya, D. Frolov, R. van Grondelle, J. P. Dekker, *Biochim. Biophys. Acta BBA—Bioenerg.* **2004**, *1656*, 104.
- [26] M. Fox, *Quantum Optics: An Introduction*, Oxford University Press, New York **2006**.
- [27] J. A. Hutchison, T. Schwartz, C. Genet, E. Devaux, T. W. Ebbesen, *Angew. Chem. Int. Ed.* **2012**, *51*, 1592.
- [28] J. Dintinger, S. Klein, F. Bustos, W. L. Barnes, T. W. Ebbesen, *Phys. Rev. B* **2005**, *71*, 035424-1 - 035424-5.
- [29] K. A. Atlasov, K. F. Karlsson, A. Rudra, B. Dwir, E. Kapon, *Opt. Express* **2008**, *16*, 16255.
- [30] A. Junginger, F. Wackenhut, A. Stuhl, F. Blendinger, M. Brecht, A. J. Meixner, *Opt. Express* **2020**, *28*, 485.
- [31] R. S. Knox, B. Q. Spring, *Photochem. Photobiol.* **2003**, *77*, 497.
- [32] P. Jordan, P. Fromme, H. T. Witt, O. Klukas, W. Saenger, N. Krauß, Three-dimensional structure of cyanobacterial photosystem I at 2.5 Å resolution. **2001**, *411*, 9.
- [33] Y. Umena, K. Kawakami, J.-R. Shen, N. Kamiya, *Nature* **2011**, *473*, 55.
- [34] A. Marais, B. Adams, A. K. Ringsmuth, M. Ferretti, J. M. Gruber, R. Hendriks, M. Schuld, S. L. Smith, I. Sinayskiy, T. P.

- J. Krüger, F. Petruccione, R. Van Grondelle, *J. R. Soc. Interface* **2018**, *15*, 20180640.
- [35] A. Konrad, M. Metzger, A. M. Kern, M. Brecht, A. J. Meixner, *Nanoscale* **2015**, *7*, 10204.
- [36] R. Rippka, R. Y. Stanier, J. Deruelles, M. Herdman, J. B. Waterbury, *Microbiology* **1979**, *111*, 1.
- [37] B. Watzler, P. Spät, N. Neumann, M. Koch, R. Sobotka, B. Macek, O. Hennrich, K. Forchhammer, *Front. Microbiol.* **2019**, *10*, 1428.
- [38] Y. Kondou, M. Nakazawa, S. Higashi, M. Watanabe, K. Manabe, *Photochem. Photobiol.* **2007**, *73*, 90.
- [39] J. T. M. Kennis, B. Gobets, I. H. M. Van Stokkum, J. P. Dekker, R. Van Grondelle, G. R. Fleming, *J. Phys. Chem. B* **2001**, *105*, 4485.
- [40] R. Lahmi, E. Sendersky, A. Perelman, M. Hagemann, K. Forchhammer, R. Schwarz, *J. Bacteriol.* **2006**, *188*, 5258.
- [41] A. Damjanović, H. M. Vaswani, P. Fromme, G. R. Fleming, *J. Phys. Chem. B* **2002**, *106*, 10251.

SUPPORTING INFORMATION

Additional supporting information may be found in the online version of the article at the publisher's website.

How to cite this article: T. Rammler, F. Wackenhut, S. zur Oven-Krockhaus, J. Rapp, K. Forchhammer, K. Harter, A. J. Meixner, *J. Biophotonics* **2022**, *15*(2), e202100136. <https://doi.org/10.1002/jbio.202100136>